Towards testing gravity with cosmic voids

Citation for published version:
Cai, YC 2018, 'Towards testing gravity with cosmic voids', International journal of modern physics d. https://doi.org/10.1142/S0218271818480073

Digital Object Identifier (DOI):
10.1142/S0218271818480073

Published In:
International journal of modern physics d

International Journal of Modern Physics D

Towards Testing Gravity with Cosmic Voids

Yan-Chuan Cai
Institute for Astronomy, University of Edinburgh, Royal Observatory, Blackford Hill
Edinburgh, EH9 3HJ, UK
cai@roe.ac.uk

Received Day Month Year
Revised Day Month Year

Cosmic void as a cosmological probe is reviewed. We introduce the theoretical background and recent development in observations of cosmic voids, focusing on its potential to test theorists of gravity. Four observables about cosmic voids are introduced: void number counts, weak gravitational lensing, redshift-space distortions and ISW around voids. We discuss opportunities on their application to current and future galaxy surveys and highlight challenges for this subject.

Keywords: Cosmology; cosmological constant; dark energy; modified gravity; cosmological models

PACS numbers:

1. Introduction

In light of the recent detection of gravitational waves from the binary neutron star merger GW170817 and simultaneous measurement of its optical counterpart GRB170817A, several popular classes of model of gravity beyond the ΛCDM are ruled out,[1–5] but many other models remain viable and would affect the growth of large-scale structure of the Universe differently, such as Brans-Dicke type theories including $f(R)$ gravity,[6] the normal-branch Dvali-Gabadadze-Porrati (nDGP) model,[7] and more complex variants of dark energy within the standard gravity. Although these surviving models such as $f(R)$ gravity and nDGP are not completely satisfactory alternative to dark energy for cosmic acceleration, the key general physical properties, the screening mechanisms[8,9] are likely to remain relevant and necessary for further development of alternative gravity models at cosmological scales. This is in part due to the fact that, by far, there is no strong evidence for a deviation from GR from solar system tests and from conventional cosmological probes of the late-time large-scale structure which focus on high-density regions of the Universe. For example, weak gravitational lensing, galaxy clustering including redshift-space distortions and cluster abundances are, in general, weighted by the locations of galaxies, which are thought to form on peaks of matter distribution. Theoretical attempts trying to explain cosmic acceleration by changing the law of gravity will have to pass tests of gravity delivered from conventional solar system tests. These stringent requirements leaves relatively little space for the development of alternative models. In essence, any viable model should converge to GR in high-density regions where most of these observations have set constraints on. This is why screening mechanism is usually needed to suppress any possible deviation from GR in those circumstances, which then leaves possible deviation from GR in the regime beyond the radar of conventional probes. For example, in large-scale cosmic voids or at the outskirt of galaxy clusters, behaviour of gravity may be allowed to be different.

At the mean time, as mentioned in Chapter 1, recent observations have indicated several low-level tensions between large-scale structure and CMB. For example, the constraints on $\Omega_m - \sigma_8$ set by weak gravitational lensing from the late-time Universe is in 2-3σ tension with constraint from CMB temperature fluctuations from Planck.[10,11] Likewise, the measurement from the brightest SZ cluster number counts seems to prefer lower ranges of $\Omega_m - \sigma_8$ than the best-fit Planck cosmology from the CMB temperature power spectrum. Perhaps the most prominent tension is the constraint for the local Hubble expansion rate H_0 delivered by CMB measurement versus that from the late-time SNe data, which is reported to be at the level of 3-4σ.[12,13] Several anomalies in the CMB have also been reported, such as the Cold Spot in the southern Galactic plane,[14,15] the alignment of quadrupole versus octopole in the CMB,[16,17] the 'power deficit' at the low-ℓ range of the CMB power spectrum,[18] and the asymmetry of clustering between the north and the south Galactic plane[19,20] – all these are confirmed by the Planck data.[21] While the reason and significance for these tensions and anomalies are disputed, i.e. it could be due to observational systematics, before they are verified or disproved by future observations or with new convincing analysis for the data, it remains possible that they indicate the imperfection of the standard model and thereby chances for new physics. There is yet not a satisfactory alternative theory of gravity which can convincingly explain those anomalies and tensions. Nonetheless, for the concern of cosmology, realising that GR being the undying governing law of gravity for the whole Universe is an assumption which comes from extrapolating the law extracted from the near-Earth environment to cosmological scales, it remains important to test the equivalence principle and GR at these scales. More generally speaking, scale is only one dimension of concern for the test of gravity. Other circumstances such as time evolution, density of local environment or the properties of local potentials are also relevant situations where the law of gravity needs to be tested.

A general feature for the surviving modified gravity models is that they often rely on screening mechanisms to suppress the fifth force in high-density regions. This is true for both the $f(R)$[22,23] and nDGP models.[7] The former features a chameleon screening and the latter the Vainshtein screening mechanism.[24,25] These non-linear behaviour of gravity inevitably alters structure formation in an environmentally dependent manner, i.e. in the regime where the fifth force is suppressed, gravity is back to GR and structure formation remains similar to that of the ΛCDM; in places where the fifth force is unscreened, such as in low density regions in the $f(R)$ model,[9,26,27] or outside the Vainshtein radius in nDGP model,[26,28] structure formation will be different due to the fifth force. This naturally leads to two branches of research in using cosmic voids to test theories of gravity: (1) on large scales, looking directly into the impact of the fifth force on the observable properties of cosmic voids; (2) at small scales, using cosmic voids as the environment for properties of dark matter haloes, galaxies or stars. This review focuses on recent research activities in the first area.

2. Cosmic voids

Cosmic voids are under-dense regions of the Universe in terms of dark matter and galaxy distribution. In principle, the distribution of voids of different sizes is related to the N-point correlation function of the density field of the Universe, and is encoded with information beyond the variance of the field. Therefore, it can be used as an alternative to characterise the nature of large-scale structure beyond the galaxy/matter two point statistics.[29–33] Moreover, the density profiles of voids encode information about cosmological model and are shaped differently by different laws of gravity. These lay the basis for why it is useful to study voids, and in general, voids and clusters for cosmology. Therefore, the evolution of individual void and the statistical distribution of voids are important to be understood.

2.1. *voids as individuals*

The evolution of individual void is addressed by the pioneering work of[34–36] with the spherical model. In the GR ΛCDM universe, the acceleration of a spherical matter

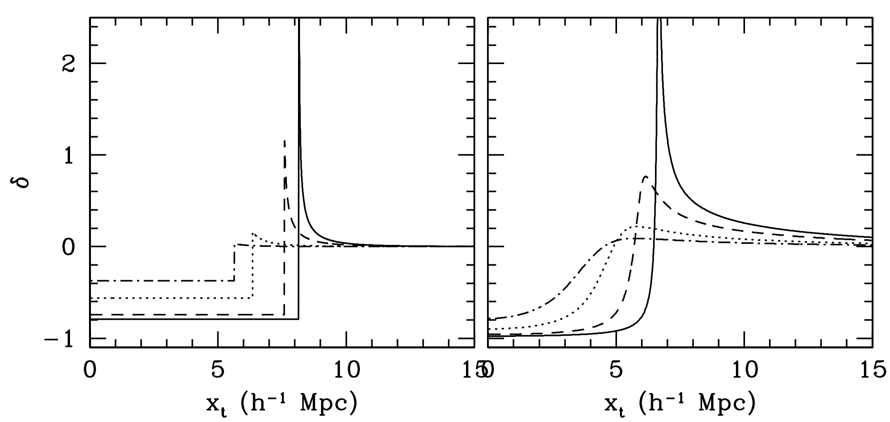

Fig. 1. Figure taken from Figure 3 of[36] The evolution of the void density profile from its initial condition till shell-crossing, starting with a spherical top-hat under-density (left) and a void with an angular averaged SCDM profile (BBKS, eqn. 7.10).[37] Different line styles represent different epochs: $a = 0.05$, 0.1, 0.2 and 0.3. See also Fig. 6 of the recent review article.[38]

shell is solely governed by the total mass within the radius r, and the background dark energy density ρ_Λ.

$$\frac{\ddot{r}}{r} = -\frac{1}{6M_{\rm Pl}^2}\left[\rho_{\rm v} - 2\rho_\Lambda\right], \tag{1}$$

where $\rho_{\rm v}$ is the mean matter density within r; ρ_Λ is the background dark energy density; $M_{\rm Pl} = 1/\sqrt{8\pi G}$ is the reduced Planck mass with G being the gravitational constant. $\dot{r}$ represents the time derivative, or velocity, and so $\ddot{r}$ is the acceleration. *If* the initial profile is a spherical top-hat under-density with radius $R_{\rm v}$, as illustrated in Fig. 1, the under-density will expand faster than the Hubble expansion. The matter shell right outside $R_{\rm v}$ will expand slightly slower than the matter shell at $R_{\rm v}$. When the inner shell overtakes the outer shell, shell crossing occurs. In an $\Omega_{\rm m} = 1$ universe, this happens when the radius of the under-density expands by a factor of 1.7, and the density contrast of the top-hat void is $\delta = -0.8$. These values have little dependence on cosmology. The depth of the top-hat void at shell-crossing has been taken as one of the conventional definitions for voids, and has been applied to predict the size distribution function of voids using the excursion set theory.[36] With more realistic initial conditions form N-body simulations, this model has been shown to be successful in tracking the evolution of void density profiles for large voids.[39]

2.2. *void distribution function*

Like the dark matter halo mass function, the statistical distribution for void population can be predicted with the excursion set theory[40] (see also Chapter 4 for more details). The basic idea of the excursion set theory is that for a Gaussian random field, the variance $S = \sigma^2(R_i)$ when smoothed by a filter of the size R_i, is specified given the linear matter power spectrum and the window function. A sequence of the density fluctuation $\delta(S)$ given by a series of increment in S, which is equivalent to decrease of the smoothing scale, follows a Brownian random walk, if the filtering of the density field is a k-space top-hat.[36,40,41] A random walk up-crossing the halo formation barrier δ_c corresponds to the formation of a halo, and one that down-crosses the void formation barrier δ_v represents a void. The probability density of a walk first crossing the barriers between $[\sigma, \sigma + d\sigma]$ is expressed as:

$$df(\sigma, \delta_{c,v}) = \frac{\delta_{c,v}}{\sigma}\sqrt{\frac{2}{\pi}}\exp\left(-\frac{\delta_{c,v}^2}{2\sigma^2}\right)\frac{d\sigma}{\sigma}, \tag{2}$$

where $\delta_c = 1.686$ for haloes and $\delta_v = -2.81$ for voids are the linearly extrapolated densities at shell-crossing, both coming from the spherical model assuming a top-hat initial density. The number density of haloes/voids as function of mass $n(M)$, or equivalently radius R_i, is then

$$\frac{dn(M)}{dM} = \frac{\bar{\rho}\; df(\sigma, \delta_{c,v})}{M dM} \tag{3}$$

where M is the mass within the spherical top-hat for either voids or haloes, and $\bar{\rho}$ is the mean matter density of the Universe. Once the linear matter power spectrum is specified, the abundance of haloes or voids can be predicted with the above equation. However, applying the above equation to void leads to violation of volume conservation. Individual voids expand as they evolve, by the time of shell-crossing, their radius would have increased by a factor of 1.7 and a factor of ~ 5 for their volume. The sum for the volumes of voids therefore exceed the total volume of the Universe. An improved version of the above model was given by Jennings et al.[42] by imposing volume conservation, with which the agreement between N-body simulation and the new model is shown to improve.[42]

It is worth noting that the shell-crossing densities mentioned above are derived from the setting that the initial condition is a spherical top-hat, which is unrealistic in the real Universe. This assumption affects the shell-crossing density for voids more than for haloes, as the former is directly related to the derivative of the initial profile and the latter is governed by the total mass within a certain radius. Therefore, it is unsurprising that the predictions for the abundance of voids from this setting does not agree very well with simulations or observations. Nonetheless, this model provides a useful guidance for the general physical picture of voids in the following aspects: (i) voids are expanding relative to the background; (ii) as voids expand, they become emptier; (iii) the distribution of voids in terms of their sizes follows some Press-Schechter-type[43] function.

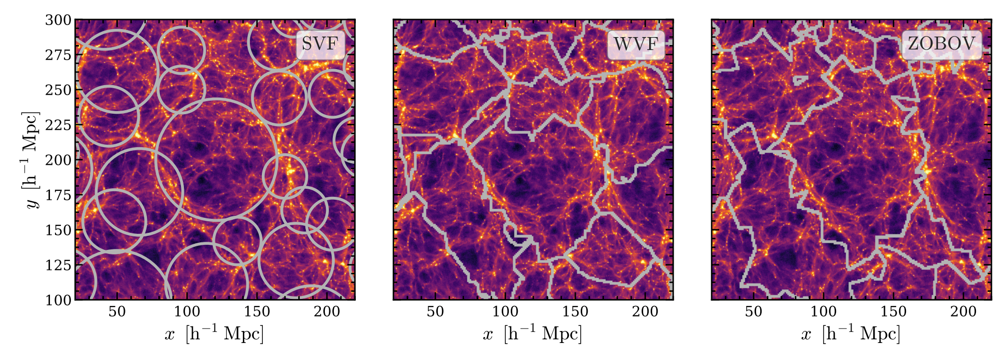

Fig. 2. Voids identified in simulations using dark matter particle distribution. Grey curves representing boundaries of voids are drawn on top of the projected density of dark matter. Three different void finding algorithms are shown for comparison: the spherical void finder,[44] the watershed void finder[45] and the ZOBOV void finder.[46] Despite some detailed differences for the exact boarders of voids, the largest void region in the simulation are consistently found by all the three algorithms.

2.3. *voids in simulation and observations*

In the real Universe, voids have complex shapes and different density profiles. Due to this nature, there is no good consensus for the definition of voids in simulations and observations. For example, there is no clear-cut answer for where the boarder of a void should be due to their irregular shapes. However, it is relatively unambiguous that they should be under dense at their centres. For example, Fig. 2 compares the void regions identified in simulations using three different void finding algorithms, the spherical void finder,[44] the watershed void finder[45] and ZOBOV.[46] We can see that despite having different boundaries, the largest voids are found in all the three different algorithms. Broadly speaking, void finding algorithms can be classified into two categories: the first uses the distribution of mater or tracers of matter to define under-dense regions, such as the three void finding algorithms mentioned above. The second uses velocity divergence to identify outflow regions, e.g.[47] Like the example give in Fig. 2, the strongest characteristic of voids being under-dense usually converges among different ways of finding voids. But the quantitative measurement for the abundance of voids as function of radius may differ significantly. This is one aspect of voids one needs to keep in mind when applying it to cosmology or astrophysics. More detailed comparisons of different algorithms can be found in.[48]

In observations, void catalogues have been generated from galaxy redshift surveys, and one of the most exploited dataset is in the SDSS area.[49–53] These have been used to study their imprints on the CMB via the Integrated Sachs-Wolfe (ISW) effect,[51, 54–63] constrain cosmology via the Alcock-Paczyński Test (AP) test,[64–67] measure the linear growth of structure[68–70] and weak gravitational lensing signal around voids[71–75] . On top of the above, there have been a number of astrophysical and cosmological applications of voids being proposed. These include: void ellipticity as a probe for the dark energy equation of state,[76–79] void abundances and profiles for testing theories of gravity[27, 80–86] and constraining neutrino masses,[87] the nature of dark matter,[88] baryon acoustic oscillations in void clustering.[89, 90] In this chapter, four observables of voids will be reviewed: void abundance, gravitational lensing of voids, redshift-space distortion around voids and ISW around voids, with a focus on their potentials to test theories of gravity.

3. The fifth force in cosmic voids

A general feature of modified gravity is that the presence of a fifth force, which changes the strength of gravity and violates the equivalence principle in certain circumstances. As shown in[24, 82, 91] for chameleon screening mechanism, violation of the equivalence principle for theories of gravity, often shown as a deviation of the inertial mass from the gravitational mass in under-dense regions, could be of the order of unity. This is also the case for the Cubic Galileon model,[86] which comes with the Vainshtein screening mechanism.[25]

In this section, we use a specific example of a coupled scalar field model to explain how the chameleon screening mechanism works in spherical structures, and illustrate how it affects large-scale structures, particularly voids. Starting from the

Lagrangian of this model

$$\mathcal{L} = \frac{1}{2}\left[M_{\rm Pl}^2 R - \nabla^a\phi\nabla_a\phi\right] + V(\phi) - C(\phi)\mathcal{L}_{\rm M}, \tag{4}$$

in which R is the Ricci scalar. $\mathcal{L}_{\rm M}$ lumps up the Lagrangian densities for dark matter and standard model species including radiation and neutrinos, except for dark energy, which in this model, is replaced by the scalar field ϕ, with $V(\phi)$ being its potential. The field is assumed to couple universally with dark matter and standard model species, characterised by the coupling function $C(\phi)$. Given the functional forms for $V(\phi)$ and $C(\phi)$, the coupled scalar field model is specified. To survive observational constraints mentioned in the introduction, the choice of these two functions for the model can be narrowed down. Qualitatively, we want the model to have the same expansion history as the ΛCDM, and to have the behaviour of gravity back to GR in high-density regions. The model investigated by[92, 93] is designed to satisfy such requirements, with

$$C(\phi) = \exp(\gamma\phi/M_{\rm Pl}), \tag{5}$$

and

$$V(\phi) = \frac{\rho_\Lambda}{\left[1 - \exp\left(-\phi/M_{\rm Pl}\right)\right]^\alpha}. \tag{6}$$

In the above ρ_Λ is a parameter of order the present dark energy density, γ, α are dimensionless parameters controlling the strength of the coupling and the steepness of the potential respectively (see Fig. 1 of[92] for an illustration of the potential).

When having $\alpha \ll 1$ and $\gamma > 0$ as in,[92, 93] which ensure that $V_{\rm eff}(\phi)$ has a global minimum close to $\phi = 0$ and that $\mathrm{d}^2 V_{\rm eff}(\phi)/\mathrm{d}\phi^2 \equiv m_\phi^2$ at this minimum is very large in high-density regions, the above requirements are met in that: (1) ϕ is trapped close to zero throughout cosmic history so that $V(\phi) \sim \rho_\Lambda$ behaves as a cosmological constant; (2) the coupling is modulated by the local density ρ, i.e. the fifth force is strongly suppressed in high-density regions where ϕ acquires a large mass, $m_\phi^2 \gg H^2$ (H is the Hubble expansion rate), and thus the fifth force cannot propagate far. The suppression of the fifth force also happens at early times when the density of the Universe is high, which naturally ensures that the model converges to GR in the early Universe. Therefore, the fifth force is mainly active at late times and in low density regions – voids. This model has similar environmentally dependent behaviour as the scalar field model first investigated by,[24] and is an example of the chameleon models, which employs the chameleon mechanism to suppress the fifth force (see chapter 1).

The coupling of a scalar field with matter induces a fifth force, as shown by the geodesic equation for matter

$$\frac{\mathrm{d}^2\mathbf{r}}{\mathrm{d}t^2} = -\vec{\nabla}\Phi - \frac{C_\phi(\phi)}{C(\phi)}\vec{\nabla}\phi, \tag{7}$$

where $\mathbf{r}$ is the position vector, t the physical time, Φ is the Newtonian potential and $\vec{\nabla}$ is the spatial derivative; $C_\phi \equiv \mathrm{d}C/\mathrm{d}\phi$. The second term on the right hand side is the fifth force. The acceleration of a test particle is no longer solely provided by the gradient of the Newtonian potential, and part of it will be provided by the gradient of the scalar field, i.e. the fifth force.

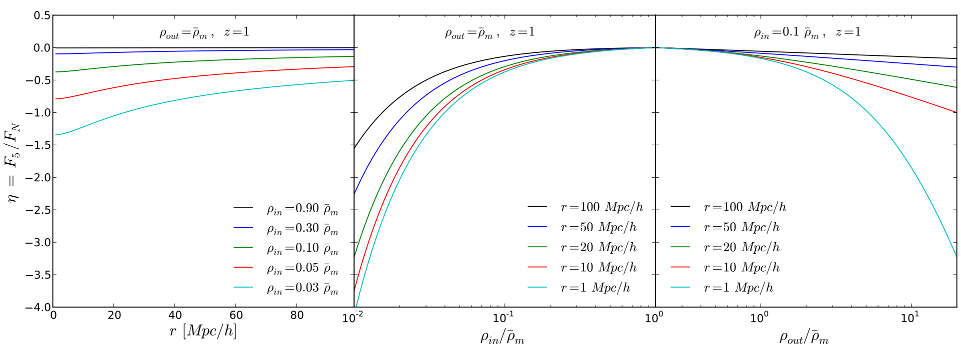

Fig. 3. Taken from Clampitt et al.[82] to illustrate the ratio between the fifth force versus Newtonian force η in the coupled scalar field model.[92,93] *Left panel:* Variations of η with the spherical top-hat radius r. The exterior density is fixed to the cosmic mean today, $\rho_{\rm out} = \bar{\rho}_m$. Various values of interior density $\rho_{\rm in}$ are shown, with $\rho_{\rm in}$ decreasing from top to bottom. *Center panel:* The same, but for continuous variations of $\rho_{\rm in}$, fixed $\rho_{\rm out} = \bar{\rho}_m$ and various values of radius r, with r decreasing from top to bottom. *Right panel:* The same, but for continuous variations of $\rho_{\rm out}$, fixed $\rho_{\rm in} = 0.1\,\bar{\rho}_m$, and various values of radius r, with r decreasing from top to bottom.

To illustrate the physics of the fifth force in voids in the above model, one can set up an isolated spherical top-hat void, solve for its corresponding scalar field profile, and compute the profiles of the fifth-force. This has been been detailed in,[82] and summarised here. The evolution equation of the spherical underdensity (void) is the key relevant equation. In this model, it can be written as

$$\frac{\ddot{r}}{r} = -\frac{1}{6M_{\rm Pl}^2}\left[\rho_{\rm v}(1+\eta) - 2\rho_\Lambda\right], \tag{8}$$

which differs from Eq. (1) by a factor of $(1+\eta)$, where η is the ratio between the fifth force and Newtonian gravity:

$$\eta = \frac{\sqrt{3\alpha\Omega_\Lambda}\gamma\frac{{\rm d}\psi}{{\rm d}\tau}\Big|_{\tau=r/\lambda_{\rm out}}}{\frac{1}{2}\Omega_m\left(H_0R_i\right)\left(ay_{\rm v}\right)^{-2}} \tag{9}$$

where $\psi = \phi/\phi_{out}$ and τ is the distance from the void centre normalised by the Compton wavelength of the scalar field at the background, $\lambda_{\rm out}$. The above equation can be solved iteratively with Eq. (8). This can be done for the entire density profile. Examples of the fifth force versus Newtonian force profile is shown in Fig. 3. A general feature for the chameleon model is that the fifth force is pointing outwards from the void centre, which will accelerate the expansion of voids, making them grow larger and deeper than their GR counterparts, as shown by the top and middle columns of Fig. 4. It is worth noting that for the same under-density, the expansion velocity of the matter shell is larger in the chameleon model than in GR, due to the larger acceleration it has been experiencing via equation (8).

From this physical picture, the following four observables are expected which can be used to test the effect of the fifth force.

• The fact that voids grow larger in chameleon models also means that they become emptier. The difference of matter distribution can be measured via gravitational lensing of voids. Perhaps more importantly, for models where there is order-of-unity difference between the lensing potential and the Newtonian potential, the gravitational lensing effect will respond to it directly, with potentially significant deviation from GR for the expected lensing signal. These will be addressed in Section 4.2.

• The fact the voids expand faster in chameleon models suggests that the velocity field around voids may provide a smoking gun to test these models. Moreover, since the velocity is the first time integral of acceleration, it responses more sensitively to the onset of the fifth force than the density field does. The information about

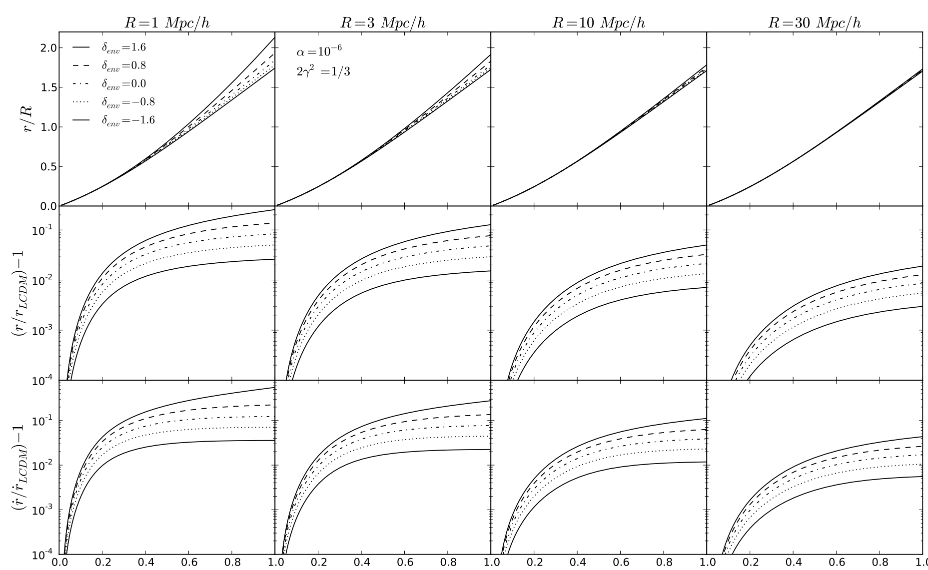

Fig. 4. Taken from Clampitt et al.[82] to illustrate the evolution of voids in the coupled scalar field model.[92,93] *Top row:* void radius r in units of its initial comoving radius R, as a function of scale factor a. *Center row:* Fractional difference between the void radii in the coupled scalar field model versus their GR version of the same initial conditions. *Bottom row:* Fractional difference in the velocity. Columns show various values of initial comoving radius, $R = 1, 3, 10$ and $30\,\mathrm{Mpc}/h$, from left to right. Different values of the exterior density are shown, with $\delta_{\rm env}$ decreasing from top to bottom. The largest deviations from GR occur for voids expanding within a larger overdense region.

the velocity field is contained naturally in the void-galaxy correlation function in redshift space, i.e. redshift-space distortion around voids. This will be discussed in Section 4.3.

• The difference for the evolution of individual voids also lead to statistical differences for the void population. One may expect small voids to merge and form larger voids, which will change the distribution function of the size of voids. The rate it occurs will be affected by the presence of a fifth force and lead to changes of the void population. Counting the number of voids as a function of their size is therefore another probe that can be used to test theories of gravity, which will be detailed in Section 4.1.

• The fact that the fifth force is suppressed in high-density regions and active in under-dense regions opens up a series of tests by comparing astrophysical phenomena in over-dense and under-dense regions and looking for the differences.[91,94–97] For example, the properties of dark matter haloes or galaxy clusters and groups, galaxies, gas and stars components in galaxies may all be different in different environment due to the fifth force.

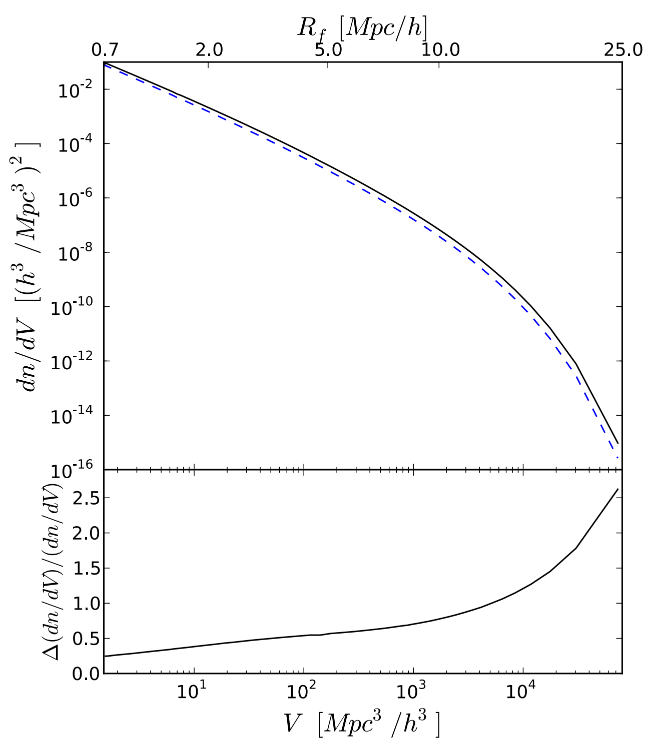

Fig. 5. From Clampitt et al.,[82] top-panel, comparing the void number counts as a function of their radius/volume between the coupled scalar field model (solid line) and the GR ΛCDM model (blue-dashed line). The bottom panels shows their fractional differences.

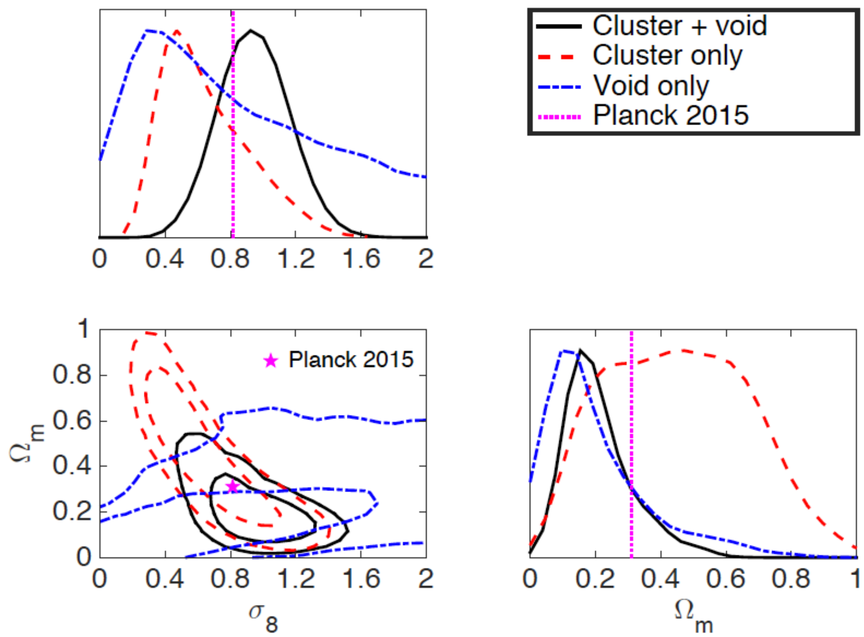

Fig. 6. From,[98] constraints on Ω_m-σ_8 for a flat ΛCDM universe using extreme value statistics with the largest void from the 2MASS-WISE galaxy catalogue and the largest cluster from the Atacama Cosmology Telescope (ACT). 68% and 95% confidence levels are shown for void (blue) and cluster (red) individually as well as for the combined case (black).

4. Observables for voids

4.1. *size distribution function of voids*

Using the well-developed excursion set theory mentioned in Section 2.2, one can predict the number of voids passing a density threshold for GR and modified gravity models. Note however, if one takes shell-crossing as the void formation barrier, the corresponding linearly extrapolated density δ_v in modified gravity models may not necessarily be a constant. For example, because of the screening mechanism, δ_v can depend on scale and environment density,[82,99] and in some specific cases, shell-crossing does not occur at all due to the varying strength of the fifth force along the radial direction of a void, i.e. for top-hat voids, the outer matter shell may have more rapid total acceleration than its inner shell and so the latter will not be able to catch up with the former.

Nonetheless, one can take the default GR value of $\delta_v = -2.81$ as the common void formation barrier for different models, and compare the resulting abundances to the GR version. The example for the coupled scalar field model is presented in Fig. 5. Indeed, we expect the abundance of voids to be higher than in the GR model for the range of void radius shown in the figure. It is worth noting that the difference between the chameleon model and GR in terms of void abundance is nearly a factor of 10 greater that of the difference for the halo mass function. This suggests that the abundance of voids may be more sensitive than haloes for constraining theories of gravity. Predictions for the $f(R)$ and Symmetron models from N-body simulations by[99] qualitatively confirms this. Although, it was also shown that when (mock) galaxies are used to define voids, it becomes more difficult to distinguish different models.[99]

A major challenge in using void abundance to test gravity is the ambiguity of void definition. To some extent, the conclusion may depend on the sample of galaxies and the specific void finding algorithm used to find voids. This leaves space for comparing different methods to find the best signal-to-noise for distinguishing different models. To overcome this challenge, mock galaxy catalogues have been employed to compare with data. As a consistency test, agreements have been found between the simulated void abundance with a fixed ΛCDM cosmology versus data from the SDSS CMASS galaxy catalogue,[52,63] although, a $\sim 3\sigma$ tension between data and simulation was noted in.[52] This may turn out to be another statistical fluke or due to unknown observational systematics. Future survey such as DESI[100] with its much larger survey volume will be able to tell more decisively if the tension remains.

The abundance of voids and clusters have also been combined to study cosmology. Using the extreme values statistics on the largest void from the 2MASS-WISE galaxy catalogue and cluster from the Atacama Cosmology Telescope (ACT), Sahlén et al.[98] were able to set constraints on Ω_m-σ_8 for a flat ΛCDM universe, as shown in Fig. 6. It has also been demonstrated that combining void abundance with cluster abundance is a powerful way to break degeneracies among cosmological parameters and potentially offers tighter constraints on modified gravity via the linear growth rate index γ from $f = \Omega_m^{\gamma}$.[101] γ is shown to be confined within a narrow range of $\gamma \approx 0.55$ in GR.[102].

4.2. *lensing around voids*

For individual voids, the density profile of voids will be altered by the presence of a fifth force. This can be measured using gravitational lensing around these objects. Weak gravitational lensing by large-scale structure of the Universe has been well studied via cosmic shear, γ, the distortions of background galaxy images by the foreground structures. This signal can be thought of being contributed by the lensing signal from peaks and troughs of the density field, and is sourced by the lensing potential

$$\psi_{\rm lens} = \frac{1}{c^2} \int \frac{D_{ls}}{D_s D_l} (\Phi + \Psi) dz, \tag{10}$$

with Φ and Ψ being the time part and space part of the metric potentials in the perturbed FRLW metric and z is the redshift. D_l, D_{ls} and D_s are the line-of-sight angular diameter distances of the lens, the source and that between the lens and the source respectively. The 2D Laplacian of the lensing potential is related to the lensing convergence κ via $\kappa = \frac{1}{2}\nabla^2\psi_{\rm lens}$. In the GR limit where $\Phi = \Psi$, it can be expressed as

$$\kappa = \frac{3H_0^2\Omega_m}{2c^2}\int \frac{D_l D_{ls}}{D_s}\frac{\delta}{a}dz. \tag{11}$$

The lensing convergence is therefore related to the projected mass density along the line of sight. It is related to the tangential component of the shear γ_t via

$$\gamma_t(R_p) = \kappa(< R_p) - \kappa(R_p) = [\Sigma(< R_p) - \Sigma(R_p)]/\Sigma_{\rm crit}, \tag{12}$$

where $\kappa(R_p)$ and $\Sigma(R_p)$ are the convergence and projected mass density at the projected radius R_p; $\kappa(< R_p)$ and $\Sigma(< R_p)$ are the averaged convergence and projected mass density within R_p (see Figs. 7 & 8 for examples). $\Sigma_{\rm crit} = \frac{c^2}{4\pi G}\frac{D_s}{D_{ls}D_l}$ is the geometry factor. The density profiles of voids (or clusters) can then be measured by stacking the shear signal of the background galaxies around them. Like galaxy-galaxy lensing, this usually requires identifying voids using 3D positions of galaxies and having lensing source galaxies behind the voids – a lensing survey overlapping with a spectroscopic redshift survey. Attempts have been made to identify voids using lensing photo-z surveys alone,[75, 103] or to measure the projected under densities on the sky plane.[104–108] The first forecast for the detectability of void lensing via stacking was made by Krause et al.[71] and Higuchi et al.[72] Detections of void lensing signal has been achieved by[73, 74] in the SDSS area and the DES science verification data.[75] CMB lensing of voids has also been detected by.[63, 109] These detections paves the way for using the signal to test theories of gravity using future galaxy redshift surveys and lensing surveys.

For chameleon models which have not been ruled out such as $f(R) gravity$,[110] the effect of the scalar field on the lensing potential is minor and so the lensing signal is unchanged if the density profile of voids are the same. In these models, the fifth force affects the lensing signal indirectly via the change of the dark matter density profile (Fig. 7). For the Galileon models (or massive gravity model), which comes with the Vainshtein screening mechanism, the relation between the lensing potential and the density perturbation can be strongly modified and the lensing signal around voids can be very different even the mass density profile is the same as in GR. For example, in the Cubic Galileon model, the lensing effects around voids of the same profiles as in GR can be a factor of two larger,[86, 111] see Fig. 8. The difference is dominated by the direct effects of the fifth force on the lensing signal.[86] For this kind of model, lensing of voids is potentially one of the most powerful probes to distinguish them from GR. Even the Galileon model has been ruled out,[112] it remains interesting for the community to explore this possibility for compelling models of this kind. It is also worth noting that for the Cubic and Quartic Galileon model, no solution for the scalar field can be found in deep voids at the late time,[113] which is a caveat for the model. This problem persist even when the the quasi-static approximation is dropped.[114]

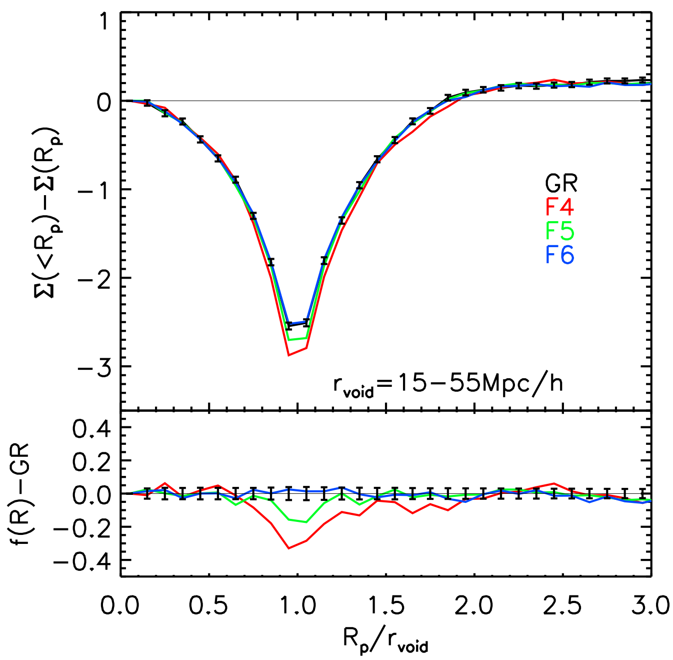

Fig. 7. From Cai et al.,[27] the lensing tangential shear profiles around voids identified in N-body simulations of ΛCDM model and $f(R)$ models, with increasing strength deviation from GR labels as F6, F5 and F4. The bottom panels shows the differences from GR. $\Sigma(< R_p) - \Sigma(R_p)$ is proportional to the surface mass density within the projected radius of R_p to which we subtract the surface mass density at R_p.

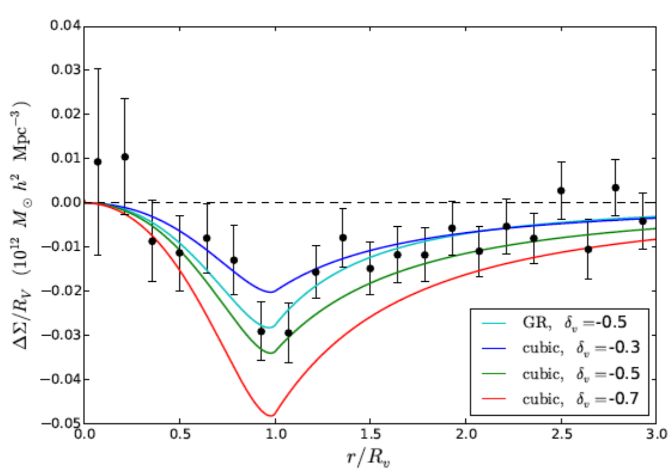

Fig. 8. From Baker et al.,[111] the observed lensing tangential shear profiles (data points with errors) around SDSS voids and SDSS LRG galaxy image data. Colour lines are model predictions from GR and the Cubic Galileon model with different void central density.

In observations, lensing signal around voids is usually sample-variance limited,[71,72,115] i.e. the signal-to-noise can be improved by having larger survey areas. The measurement is best conducted with a lensing survey over the same area as a spectroscopic survey, within which voids can be identified using the 3D positions of galaxies (although 2D voids can also be identified with a lensing survey alone with photo-z, see[75]). Near future surveys such as LSST and Euclid will meet such a requirement for at least part of their areas. A recent forecast for the detectability of the $f(R)$ model has been made in,[115] finding that the distinguishing power with LSST and Euclid is still limited to $F5$, which is compatible to other cosmological tests over similar scales[115] (see Table 1 of Lombriser (2014)[116] and references therein). With a similar survey setting and using 3D voids, the constraining power for the nDGP model is found to be somewhat weaker.[117]

A recent development on lensing around voids has generalised the idea to troughs, which is to measure the lensing signal around under densities in the projected galaxy field.[104–107] This has the advantage over the 3D void method for the following reasons: (1) identifying troughs in projected galaxy density field does not require 3D positions of galaxies, therefore, a lensing survey alone allows the measurement to be conducted. (2) An analytical model to predict the signal has been developed in,[104,107] which allows the constraints on cosmology, and possible extensions to modified gravity. (3) The lensing signal around troughs can be much stronger than 3D voids if one chooses a relatively small size for the troughs (or aperture), although the price to pay is that the difference between GR and modified gravity may be weaker due to the projection effect. In a recent study by Cautun et al,[115] it has been shown that in their specific setting, the distinguishing power for $f(R)$ vs GR is indeed greater using troughs than using 3D voids. Note that the conclusion of Cautun et al. may not necessarily apply to other settings of galaxy surveys and lensing surveys. It remains important to investigate the optimal distinguishing power for testing gravity for specific surveys.

4.3. *redshift-space distortions around voids*

While gravitational lensing probes the sum of the two metric potentials, the motion of galaxies usually responses only to the Newtonian potential. The combination of lensing and kinematic measurement such as redshift-space distortions can be used to test the gravitational slip.[118–123] This applies to voids, where the gravitational slip may be the strongest.[124]

Redshift-space distortions (RSD) arise from the fact that the observed distance of a galaxy s is perturbed by its peculiar velocity along the line of sight $v_{\rm pec}$:

$$s = r + v_{\rm pec}/(aH), \tag{13}$$

where r is the real space comoving distances of a galaxy, a is the scale factor of the Universe and H is the Hubble constant. On large scales, infall motion of galaxies towards high-density regions causes the amplitudes of galaxy clustering to increase along the line of sight. The galaxy two point correlation function appears flattened along the line of sight. For voids, we expect to have coherent outflow velocities around void centres, but the expected distortion pattern is not simply the opposite of the case in high-density regions. Several studies have developed and tested models for RSD around voids in the standard ΛCDM model[68, 125–127] in order to extract the growth rate. At the linear order, the redshift-space void-galaxy correlation function is

$$\xi^s(\mathbf{r}) = \xi^r(r) + \frac{1}{3}\beta\bar{\xi}^r(r) + \beta\mu^2[\xi^r(r) - \bar{\xi}^r(r)], \tag{14}$$

where $\mu = \cos\theta$ and θ is the subtended angle from the line of sight; $\beta = f/b$ and $f = d\ln D/d\ln a$ is the linear growth rate with D being the linear growth factor and b is the linear galaxy bias. ξ^r is the real space void-galaxy correlation function.

In this model, the void-galaxy correlation function may be flattened or elongated depending on the real space density profile of voids, and its corresponding velocity profile[68] (see Fig. 9 for an example). Linear theory applies to regions where the density fluctuation is small, which may not be the case near the centre of voids. As shown in Nadathur et al.,[126] the distortion patten with a second order term included may differ from the linear model (see[126] for an expression where some higher order terms are kept). This is also hinted by the study of Achitouv & Cai.[128] They have shown that in regions where the local density is significantly lower than the mean density, the growth rate is non-linear. This suggests that more sophisticated model may be needed to fully describe the distortion patterns near the void centre. This has been a topic of active investigation in recent years, with some noticeable theoretical problems and debates not fully resolved in GR. I listed a few of them here: (1) to what accuracy the galaxy bias around voids remains linear; (2) to what accuracy the mapping between density and velocity around voids remains linear. Nonetheless, an accurate modelling for the distortion pattens induced by peculiar velocities can be used to constrain the growth of structure.

RSD around voids encodes information about the density and velocity. This is ideal for capturing the difference between GR and non-standard gravity models, where violation of the equivalence principle may occur most evidently in voids. The fact that voids become deeper in chameleon models will show as a higher amplitude of monopole in the void-galaxy correlation function in real space. This effect will be enhanced further when observing voids in redshift space because of the larger amplitudes of expansion velocity around voids. Therefore, RSD around voids is a promising observable which can capture the combination of these two effects.[27, 68] The linear model can be used as a consistency check for deviations from GR. It has been demonstrated in[68] that the linear growth rate can be recovered using RSD around voids.

Observational constrains for the growth rate parameter using RSD around voids have been reported by Achitouv et al.[129] from the 6dF Galaxy Survey, Hawken et al.[130] from the VIPERS survey and Hamaus et al.[69, 70] using SDSS void catalogues. Among them, a somewhat lower growth rate was found at $z \sim 0.7$ from the VIPERS results than from other constraints from other measurements (Fig. 12 in the paper), though not significant. Also, at lower redshift, there is a $2-3\sigma$ tension with GR from the SDSS low-z sample,[70] as shown in Fig. 10. These may indicate an imperfection of current linear model, or a tension with general relativity. One also needs to caution the possible imperfect calibration of survey systematics in the SDSS area.[131]

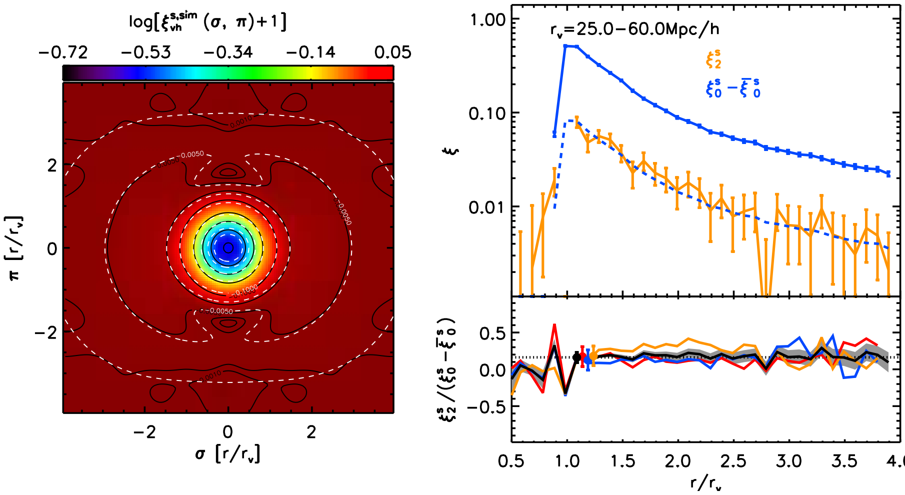

Fig. 9. From Cai et al.,[68] left: comparing the the void-halo correlation function in redshift space measured from simulations with the linear theory. The black contours give results from the simulation and the white contours are the best-fit linear model. Right: the upper panel shows the monopole and quadrupole moments of the correlation function. The black curve is from taking all measurements of voids along three different major axes of the simulation box, with the shaded region showing the error on the mean. The other three curves represent results from viewing the simulation along three different major axes. The black filled circle with error bars is the best-fit value from viewing voids along three different directions. The red, blue and orange filled circles and errors are from individual viewing directions. They are slightly offset from each other to aid visibility.

4.4. *ISW signal from voids and superclusters*

The Integrated Sachs-Wolfe (ISW) effect[54] is a CMB secondary effect which arises from the evolution of large-scale gravitational potentials. In the ΛCDM universe, dark energy stretches cosmic voids and superclusters, causing their gravitational potentials to decay. Photons from the CMB will lose/gain energy when traversing a void/supercluster, and so the CMB temperature is expected to be colder/hotter when a void/supercluster sits along the line of sight. The induced temperature fluctuations are

$$\frac{\Delta T}{T_{\rm CMB}} = -\frac{1}{c^2}\int(\dot{\Phi}+\dot{\Psi})dt, \tag{15}$$

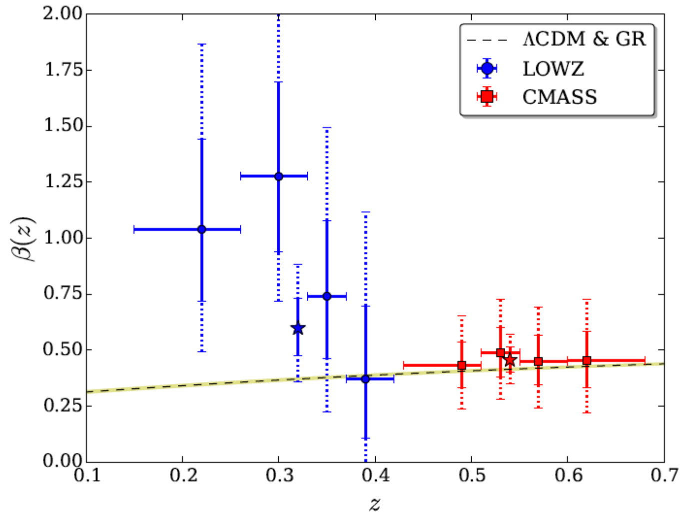

Fig. 10. From Hamaus et al.,[70] constraints on the growth rate pamameter $\beta(z) = f(z)/b(z)$ using void-galaxy correlation functions from the SDSS LOWZ (blue circles) and CMASS (red squares) galaxy samples. Stars represent the joint constraint from voids of all redshifts in each sample. Vertical solid lines indicate one and two σ errors. The dashed line with yellow shading shows fiducial GR ΛCDM model with the linear bias $b = 1.85$. The tow data points at the lowest redshifts are not fully consistent with the model line.

where the $\dot{\Phi}$ and $\dot{\Psi}$) are the time derivative of the metric potentials and $T_{\rm CMB}$ is the CMB temperature. The signal is sensitive to the time variation of the metric potentials, and its detection would give direct evidence for dark energy and can be used to constrain theories of gravity.[120,132] In the standard model, the signal is expected to be much smaller than the primordial CMB temperature fluctuation, posing a challenge for its direct detection. Therefore, cross-correlation between galaxy samples with the CMB is usually employed to extract the signal. A $\sim 4\sigma$ detection of the signal has been reported by combining multiple galaxy samples and cross-correlate them with the CMB,[133,134] and these have placed constraints for the chameleon models.[120,132]

Another way to detect the signal is by stacking the CMB with voids and superclusters found in the late-time large-scale structure. This should yield a cold and hot spot respectively for voids and superclusters. It was first conducted by Granett et al.[55] where a somewhat unexpected high significant ($\sim 4\sigma$) result was reported by stacking superstructures found form the photo-z galaxy catalogue in the SDSS area.

However, the amplitudes of the signal were higher than expected from the standard model. Follow up analysis using similar method with spectroscopic redshift catalogue (but still in the SDSS area) confirms the results qualitatively,[51,56–61,63,135] which may indicate a tension with the standard model, but the study by Nadathur & Crittenden[62] has found an agreement with the ΛCDM model when using a (different) matched filter approach.

While the debate over the amplitudes and significance of the stacked ISW signal around voids and superclusters may continue, all the above studies have found that the sign of the ISW signal to be consistent with expectation from the standard model. These analysis, together with the positive cross-correlation between the entire galaxy sample with the CMB, strongly indicate that the late-time large-scale potentials are indeed decaying. This has placed the strongest constraints for the Galileon model.[112] Combining superstructures from galaxy surveys which cover a different area from the SDSS should be able to beat down the statistical error and hence help to settle the debate and provide better constraints for cosmology.

5. Summary and notes for the future

Observables of cosmic voids focus on low density regions of the Universe. They are potentially powerful for testing theories of gravity where violation of the equivalence principle is expected to occur most prominently in low density regions. A common reason behind this is that void statistics such as abundance, void lensing and RSD are sensitive to the non-Gaussianity of the density field, which is expected to be different in modified gravity models than in GR.

Using the four observables about voids mentioned above, some level of tension or inconsistency for cosmological constraints have been reported, in contrast to the constrains from conventional methods such as two-point statistics. For example, both the void abundance and void RSD analysis using SDSS data have indicated some level of tension with the standard ΛCDM model,[52,70] which is not seen in most of the SDSS analysis using galaxy clustering. We know that there are observational systematics such as star contamination and galactic extinction in the SDSS data.[131,136,137] Although they have been calibrated to meet the precision requirements needed for galaxy clustering, it is unclear if such systematic calibration is sufficient for the relevant void statistics.

Therefore, while these new analysis using voids may open up windows for new physics, one needs to be cautious about possible effect from uncharted observational systematics. Next generation galaxy surveys such as DESI, LSST and Euclid promises to increase the current survey volume and number of galaxies by an order of magnitude. The statistical errors of these measurements will go down substantially, and so the control over systematic errors for galaxy surveys will be paramount. Calibration of observational systematics will likely to remain the major challenge for constraining theories of gravity using large-scale structure.

Facing this challenge, it is perhaps more pressing to employ novel cosmological probes and new methods of data analysis. Given that different probes may suffer from different systematics, using multiple probes will allows them to be cross-checked with each other and deliver more stringent results.

Acknowledgments

YC was supported by supported by the European Research Council under grant numbers 670193. YC thank Baojiu Li and Vasiliy Demchenko for useful comments.

References

1. L. Lombriser and A. Taylor, *jcap* **3** (March 2016) 031, hrefhttp://arxiv.org/abs/1509.08458arXiv:1509.08458.
2. T. Baker, E. Bellini, P. G. Ferreira, M. Lagos, J. Noller and I. Sawicki, *ArXiv e-prints* (October 2017) hrefhttp://arxiv.org/abs/1710.06394arXiv:1710.06394.
3. J. Sakstein and B. Jain, *ArXiv e-prints* (October 2017) hrefhttp://arxiv.org/abs/1710.05893arXiv:1710.05893.
4. J. María Ezquiaga and M. Zumalacárregui, *ArXiv e-prints* (October 2017) hrefhttp://arxiv.org/abs/1710.05901arXiv:1710.05901.
5. P. Creminelli and F. Vernizzi, *ArXiv e-prints* (October 2017) hrefhttp://arxiv.org/abs/1710.05877arXiv:1710.05877.
6. A. De Felice and S. Tsujikawa, *Living Reviews in Relativity* **13** (June 2010) 3, hrefhttp://arxiv.org/abs/1002.4928arXiv:1002.4928 [gr-qc].
7. G. Dvali, G. Gabadadze and M. Porrati, *Physics Letters B* **484** (June 2000) 112, hrefhttp://arxiv.org/abs/hep-th/0002190hep-th/0002190.
8. P. Brax, *Classical and Quantum Gravity* **30** (November 2013) 214005.
9. B. Falck, K. Koyama and G.-B. Zhao, *jcap* **7** (July 2015) 049, hrefhttp://arxiv.org/abs/1503.06673arXiv:1503.06673.
10. H. Hildebrandt, M. Viola, C. Heymans, S. Joudaki, K. Kuijken, C. Blake, T. Erben, B. Joachimi, D. Klaes, L. Miller, C. B. Morrison, R. Nakajima, G. Verdoes Kleijn, A. Amon, A. Choi, G. Covone, J. T. A. de Jong, A. Dvornik, I. Fenech Conti, A. Grado, J. Harnois-Déraps, R. Herbonnet, H. Hoekstra, F. Köhlinger, J. McFarland, A. Mead, J. Merten, N. Napolitano, J. A. Peacock, M. Radovich, P. Schneider, P. Simon, E. A. Valentijn, J. L. van den Busch, E. van Uitert and L. Van Waerbeke, *MNRAS* **465** (February 2017) 1454, hrefhttp://arxiv.org/abs/1606.05338arXiv:1606.05338.
11. DES Collaboration, T. M. C. Abbott, F. B. Abdalla, A. Alarcon, J. Aleksić, S. Allam, S. Allen, A. Amara, J. Annis, J. Asorey, S. Avila, D. Bacon, E. Balbinot, M. Banerji, N. Banik, W. Barkhouse, M. Baumer, E. Baxter, K. Bechtol, M. R. Becker, A. Benoit-Lévy, B. A. Benson, G. M. Bernstein, E. Bertin, J. Blazek, S. L. Bridle, D. Brooks, D. Brout, E. Buckley-Geer, D. L. Burke, M. T. Busha, D. Capozzi, A. Carnero Rosell, M. Carrasco Kind, J. Carretero, F. J. Castander, R. Cawthon, C. Chang, N. Chen, M. Childress, A. Choi, C. Conselice, R. Crittenden, M. Crocce, C. E. Cunha, C. B. D'Andrea, L. N. da Costa, R. Das, T. M. Davis, C. Davis, J. De Vicente, D. L. DePoy, J. DeRose, S. Desai, H. T. Diehl, J. P. Dietrich, S. Dodelson, P. Doel, A. Drlica-Wagner, T. F. Eifler, A. E. Elliott, F. Elsner, J. Elvin-Poole, J. Estrada, A. E. Evrard, Y. Fang, E. Fernandez, A. Ferté, D. A. Finley, B. Flaugher, P. Fosalba, O. Friedrich, J. Frieman, J. García-Bellido, M. Garcia-Fernandez, M. Gatti, E. Gaztanaga, D. W. Gerdes, T. Giannantonio, M. S. S. Gill, K. Glazebrook, D. A. Goldstein, D. Gruen, R. A. Gruendl, J. Gschwend, G. Gutierrez, S. Hamilton, W. G.

Hartley, S. R. Hinton, K. Honscheid, B. Hoyle, D. Huterer, B. Jain, D. J. James, M. Jarvis, T. Jeltema, M. D. Johnson, M. W. G. Johnson, T. Kacprzak, S. Kent, A. G. Kim, A. King, D. Kirk, N. Kokron, A. Kovacs, E. Krause, C. Krawiec, A. Kremin, K. Kuehn, S. Kuhlmann, N. Kuropatkin, F. Lacasa, O. Lahav, T. S. Li, A. R. Liddle, C. Lidman, M. Lima, H. Lin, N. MacCrann, M. A. G. Maia, M. Makler, M. Manera, M. March, J. L. Marshall, P. Martini, R. G. McMahon, P. Melchior, F. Menanteau, R. Miquel, V. Miranda, D. Mudd, J. Muir, A. Möller, E. Neilsen, R. C. Nichol, B. Nord, P. Nugent, R. L. C. Ogando, A. Palmese, J. Peacock, H. V. Peiris, J. Peoples, W. J. Percival, D. Petravick, A. A. Plazas, A. Porredon, J. Prat, A. Pujol, M. M. Rau, A. Refregier, P. M. Ricker, N. Roe, R. P. Rollins, A. K. Romer, A. Roodman, R. Rosenfeld, A. J. Ross, E. Rozo, E. S. Rykoff, M. Sako, A. I. Salvador, S. Samuroff, C. Sánchez, E. Sanchez, B. Santiago, V. Scarpine, R. Schindler, D. Scolnic, L. F. Secco, S. Serrano, I. Sevilla-Noarbe, E. Sheldon, R. C. Smith, M. Smith, J. Smith, M. Soares-Santos, F. Sobreira, E. Suchyta, G. Tarle, D. Thomas, M. A. Troxel, D. L. Tucker, B. E. Tucker, S. A. Uddin, T. N. Varga, P. Vielzeuf, V. Vikram, A. K. Vivas, A. R. Walker, M. Wang, R. H. Wechsler, J. Weller, W. Wester, R. C. Wolf, B. Yanny, F. Yuan, A. Zenteno, B. Zhang, Y. Zhang and J. Zuntz, *ArXiv e-prints* (August 2017) hrefhttp://arxiv.org/abs/1708.01530arXiv:1708.01530.

12. A. G. Riess, S. Casertano, W. Yuan, L. Macri, J. Anderson, J. W. MacKenty, J. B. Bowers, K. I. Clubb, A. V. Filippenko, D. O. Jones and B. E. Tucker, *ApJ* **855** (March 2018) 136, hrefhttp://arxiv.org/abs/1801.01120arXiv:1801.01120 [astro-ph.SR].
13. A. G. Riess, S. Casertano, W. Yuan, L. Macri, B. Bucciarelli, M. G. Lattanzi, J. W. MacKenty, J. B. Bowers, W. Zheng, A. V. Filippenko, C. Huang and R. I. Anderson, *ArXiv e-prints* (April 2018) hrefhttp://arxiv.org/abs/1804.10655arXiv:1804.10655.
14. P. Vielva, E. Martínez-González, R. B. Barreiro, J. L. Sanz and L. Cayón, *ApJ* **609** (July 2004) 22, hrefhttp://arxiv.org/abs/astro-ph/0310273astro-ph/0310273.
15. M. Cruz, E. Martínez-González, P. Vielva and L. Cayón, *MNRAS* **356** (January 2005) 29, hrefhttp://arxiv.org/abs/astro-ph/0405341astro-ph/0405341.
16. M. Tegmark, A. de Oliveira-Costa and A. J. Hamilton, *Phys. Rev. D* **68** (December 2003) 123523, hrefhttp://arxiv.org/abs/astro-ph/0302496astro-ph/0302496.
17. D. J. Schwarz, G. D. Starkman, D. Huterer and C. J. Copi, *Physical Review Letters* **93** (November 2004) 221301, hrefhttp://arxiv.org/abs/astro-ph/0403353astro-ph/0403353.
18. Planck Collaboration, P. A. R. Ade, N. Aghanim, C. Armitage-Caplan, M. Arnaud, M. Ashdown, F. Atrio-Barandela, J. Aumont, C. Baccigalupi, A. J. Banday and et al., *A&A* **571** (November 2014) A15, hrefhttp://arxiv.org/abs/1303.5075arXiv:1303.5075.
19. H. K. Eriksen, A. J. Banday, K. M. Górski, F. K. Hansen and P. B. Lilje, *ApJ* **660** (May 2007) L81, hrefhttp://arxiv.org/abs/astro-ph/0701089astro-ph/0701089.
20. F. K. Hansen, A. J. Banday, K. M. Górski, H. K. Eriksen and P. B. Lilje, *ApJ* **704** (October 2009) 1448, hrefhttp://arxiv.org/abs/0812.3795arXiv:0812.3795.
21. Planck Collaboration, P. A. R. Ade, N. Aghanim, C. Armitage-Caplan, M. Arnaud, M. Ashdown, F. Atrio-Barandela, J. Aumont, C. Baccigalupi, A. J. Banday and et al., *A&A* **571** (November 2014) A23, hrefhttp://arxiv.org/abs/1303.5083arXiv:1303.5083.
22. B. Li and J. D. Barrow, *Phys. Rev.* **D75** (2007) 084010, hrefhttp://arxiv.org/abs/gr-qc/0701111arXiv:gr-qc/0701111 [gr-qc].
23. P. Brax, C. van de Bruck, A.-C. Davis and D. J. Shaw, *Phys. Rev.* **D78** (2008) 104021, hrefhttp://arxiv.org/abs/0806.3415arXiv:0806.3415 [astro-ph].
24. J. Khoury and A. Weltman, *Phys. Rev. D* **69** (February 2004) 044026,

hrefhttp://arxiv.org/abs/astro-ph/0309411astro-ph/0309411.
25. A. Vainshtein, *Physics Letters B* **39** (1972) 393 .
26. F. Schmidt, *Phys. Rev. D* **81** (May 2010) 103002, hrefhttp://arxiv.org/abs/1003.0409arXiv:1003.0409 [astro-ph.CO].
27. Y.-C. Cai, N. Padilla and B. Li, *MNRAS* **451** (July 2015) 1036, hrefhttp://arxiv.org/abs/1410.1510arXiv:1410.1510.
28. B. Falck, K. Koyama, G.-b. Zhao and B. Li, *jcap* **7** (July 2014) 058, hrefhttp://arxiv.org/abs/1404.2206arXiv:1404.2206.
29. S. D. M. White, *MNRAS* **186** (January 1979) 145.
30. W. C. Saslaw and A. J. S. Hamilton, *ApJ* **276** (January 1984) 13.
31. A. J. S. Hamilton, *ApJ* **292** (May 1985) L35.
32. J. N. Fry, *ApJ* **289** (February 1985) 10.
33. J. N. Fry, *ApJ* **306** (July 1986) 358.
34. E. Bertschinger, *ApJS* **58** (May 1985) 1.
35. G. R. Blumenthal, L. N. da Costa, D. S. Goldwirth, M. Lecar and T. Piran, *ApJ* **388** (April 1992) 234.
36. R. K. Sheth and R. van de Weygaert, *MNRAS* **350** (May 2004) 517, hrefhttp://arxiv.org/abs/astro-ph/0311260astro-ph/0311260.
37. J. M. Bardeen, J. R. Bond, N. Kaiser and A. S. Szalay, *ApJ* **304** (May 1986) 15.
38. R. van de Weygaert, Voids and the Cosmic Web: cosmic depression & spatial complexity, in *The Zeldovich Universe: Genesis and Growth of the Cosmic Web*, eds. R. van de Weygaert, S. Shandarin, E. Saar and J. Einasto, IAU Symposium, Vol. 308 (October 2016), pp. 493–523. hrefhttp://arxiv.org/abs/1611.01222arXiv:1611.01222.
39. V. Demchenko, Y.-C. Cai, C. Heymans and J. A. Peacock, *MNRAS* **463** (November 2016) 512, hrefhttp://arxiv.org/abs/1605.05286arXiv:1605.05286.
40. J. R. Bond, S. Cole, G. Efstathiou and N. Kaiser, *ApJ* **379** (October 1991) 440.
41. A. R. Zentner, *International Journal of Modern Physics D* **16** (2007) 763, hrefhttp://arxiv.org/abs/astro-ph/0611454astro-ph/0611454.
42. E. Jennings, Y. Li and W. Hu, *MNRAS* **434** (September 2013) 2167, hrefhttp://arxiv.org/abs/1304.6087arXiv:1304.6087.
43. W. H. Press and P. Schechter, *ApJ* **187** (February 1974) 425.
44. N. D. Padilla, L. Ceccarelli and D. G. Lambas, *MNRAS* **363** (November 2005) 977, hrefhttp://arxiv.org/abs/astro-ph/0508297astro-ph/0508297.
45. E. Platen, R. van de Weygaert and B. J. T. Jones, *MNRAS* **380** (September 2007) 551, hrefhttp://arxiv.org/abs/0706.2788arXiv:0706.2788.
46. M. C. Neyrinck, *MNRAS* **386** (June 2008) 2101, hrefhttp://arxiv.org/abs/0712.3049arXiv:0712.3049.
47. Y. Hoffman, O. Metuki, G. Yepes, S. Gottlöber, J. E. Forero-Romero, N. I. Libeskind and A. Knebe, *MNRAS* **425** (September 2012) 2049, hrefhttp://arxiv.org/abs/1201.3367arXiv:1201.3367 [astro-ph.CO].
48. J. M. Colberg, F. Pearce, C. Foster, E. Platen, R. Brunino, M. Neyrinck, S. Basilakos, A. Fairall, H. Feldman, S. Gottlöber, O. Hahn, F. Hoyle, V. Müller, L. Nelson, M. Plionis, C. Porciani, S. Shandarin, M. S. Vogeley and R. van de Weygaert, *MNRAS* **387** (June 2008) 933, hrefhttp://arxiv.org/abs/0803.0918arXiv:0803.0918.
49. D. C. Pan, M. S. Vogeley, F. Hoyle, Y.-Y. Choi and C. Park, *MNRAS* **421** (April 2012) 926, hrefhttp://arxiv.org/abs/1103.4156arXiv:1103.4156.
50. P. M. Sutter, G. Lavaux, B. D. Wandelt and D. H. Weinberg, *ApJ* **761** (December 2012) 44, hrefhttp://arxiv.org/abs/1207.2524arXiv:1207.2524.
51. Y.-C. Cai, M. C. Neyrinck, I. Szapudi, S. Cole and C. S. Frenk, *ApJ* **786** (May 2014)

110, hrefhttp://arxiv.org/abs/1301.6136arXiv:1301.6136.
52. S. Nadathur, *MNRAS* **461** (September 2016) 358, hrefhttp://arxiv.org/abs/1602.04752arXiv:1602.04752.
53. Q. Mao, A. A. Berlind, R. J. Scherrer, M. C. Neyrinck, R. Scoccimarro, J. L. Tinker, C. K. McBride, D. P. Schneider, K. Pan, D. Bizyaev, E. Malanushenko and V. Malanushenko, *ApJ* **835** (February 2017) 161, hrefhttp://arxiv.org/abs/1602.02771arXiv:1602.02771.
54. R. K. Sachs and A. M. Wolfe, *ApJ* **147** (January 1967) 73.
55. B. R. Granett, M. C. Neyrinck and I. Szapudi, *APJL* **683** (August 2008) L99, hrefhttp://arxiv.org/abs/0805.3695arXiv:0805.3695.
56. S. Nadathur, S. Hotchkiss and S. Sarkar, *JCAP* **6** (June 2012) 42, hrefhttp://arxiv.org/abs/1109.4126arXiv:1109.4126 [astro-ph.CO].
57. S. Flender, S. Hotchkiss and S. Nadathur, *JCAP* **2** (February 2013) 13, hrefhttp://arxiv.org/abs/1212.0776arXiv:1212.0776 [astro-ph.CO].
58. S. Ilić, M. Langer and M. Douspis, *A&A* **556** (August 2013) A51, hrefhttp://arxiv.org/abs/1301.5849arXiv:1301.5849 [astro-ph.CO].
59. A. Kovács and B. R. Granett, *MNRAS* **452** (September 2015) 1295, hrefhttp://arxiv.org/abs/1501.03376arXiv:1501.03376.
60. Planck Collaboration, P. A. R. Ade, N. Aghanim, M. Arnaud, M. Ashdown, J. Aumont, C. Baccigalupi, A. J. Banday, R. B. Barreiro, N. Bartolo and et al., *A&A* **594** (September 2016) A21, hrefhttp://arxiv.org/abs/1502.01595arXiv:1502.01595.
61. S. Aiola, A. Kosowsky and B. Wang, *PRD* **91** (February 2015) 043510, hrefhttp://arxiv.org/abs/1410.6138arXiv:1410.6138.
62. S. Nadathur and R. Crittenden, *ApJ* **830** (October 2016) L19, hrefhttp://arxiv.org/abs/1608.08638arXiv:1608.08638.
63. Y.-C. Cai, M. Neyrinck, Q. Mao, J. A. Peacock, I. Szapudi and A. A. Berlind, *MNRAS* **466** (April 2017) 3364, hrefhttp://arxiv.org/abs/1609.00301arXiv:1609.00301.
64. C. Alcock and B. Paczynski, *Nature* **281** (October 1979) 358.
65. G. Lavaux and B. D. Wandelt, *APJ* **754** (August 2012) 109, hrefhttp://arxiv.org/abs/1110.0345arXiv:1110.0345 [astro-ph.CO].
66. P. M. Sutter, A. Pisani, B. D. Wandelt and D. H. Weinberg, *MNRAS* **443** (October 2014) 2983, hrefhttp://arxiv.org/abs/1404.5618arXiv:1404.5618.
67. Q. Mao, A. A. Berlind, R. J. Scherrer, M. C. Neyrinck, R. Scoccimarro, J. L. Tinker, C. K. McBride and D. P. Schneider, *ApJ* **835** (February 2017) 160, hrefhttp://arxiv.org/abs/1602.06306arXiv:1602.06306.
68. Y.-C. Cai, A. Taylor, J. A. Peacock and N. Padilla, *MNRAS* **462** (November 2016) 2465, hrefhttp://arxiv.org/abs/1603.05184arXiv:1603.05184.
69. N. Hamaus, A. Pisani, P. M. Sutter, G. Lavaux, S. Escoffier, B. D. Wandelt and J. Weller, *Physical Review Letters* **117** (August 2016) 091302, hrefhttp://arxiv.org/abs/1602.01784arXiv:1602.01784.
70. N. Hamaus, M.-C. Cousinou, A. Pisani, M. Aubert, S. Escoffier and J. Weller, *jcap* **7** (July 2017) 014, hrefhttp://arxiv.org/abs/1705.05328arXiv:1705.05328.
71. E. Krause, T.-C. Chang, O. Doré and K. Umetsu, *ApJ* **762** (January 2013) L20, hrefhttp://arxiv.org/abs/1210.2446arXiv:1210.2446.
72. Y. Higuchi, M. Oguri and T. Hamana, *MNRAS* **432** (June 2013) 1021, hrefhttp://arxiv.org/abs/1211.5966arXiv:1211.5966.
73. P. Melchior, P. M. Sutter, E. S. Sheldon, E. Krause and B. D. Wandelt, *MNRAS* **440** (June 2014) 2922, hrefhttp://arxiv.org/abs/1309.2045arXiv:1309.2045.
74. J. Clampitt and B. Jain, *MNRAS* **454** (December 2015) 3357,

hrefhttp://arxiv.org/abs/1404.1834arXiv:1404.1834.
75. C. Sánchez, J. Clampitt, A. Kovacs, B. Jain, J. García-Bellido, S. Nadathur, D. Gruen, N. Hamaus, D. Huterer, P. Vielzeuf, A. Amara, C. Bonnett, J. DeRose, W. G. Hartley, M. Jarvis, O. Lahav, R. Miquel, E. Rozo, E. S. Rykoff, E. Sheldon, R. H. Wechsler, J. Zuntz, T. M. C. Abbott, F. B. Abdalla, J. Annis, A. Benoit-Lévy, G. M. Bernstein, R. A. Bernstein, E. Bertin, D. Brooks, E. Buckley-Geer, A. Carnero Rosell, M. Carrasco Kind, J. Carretero, M. Crocce, C. E. Cunha, C. B. D'Andrea, L. N. da Costa, S. Desai, H. T. Diehl, J. P. Dietrich, P. Doel, A. E. Evrard, A. Fausti Neto, B. Flaugher, P. Fosalba, J. Frieman, E. Gaztanaga, R. A. Gruendl, G. Gutierrez, K. Honscheid, D. J. James, E. Krause, K. Kuehn, M. Lima, M. A. G. Maia, J. L. Marshall, P. Melchior, A. A. Plazas, K. Reil, A. K. Romer, E. Sanchez, M. Schubnell, I. Sevilla-Noarbe, R. C. Smith, M. Soares-Santos, F. Sobreira, E. Suchyta, G. Tarle, D. Thomas, A. R. Walker, J. Weller and DES Collaboration, *MNRAS* **465** (February 2017) 746, hrefhttp://arxiv.org/abs/1605.03982arXiv:1605.03982.
76. J. Lee and D. Park, *APJL* **696** (May 2009) L10, hrefhttp://arxiv.org/abs/0704.0881arXiv:0704.0881.
77. G. Lavaux and B. D. Wandelt, *MNRAS* **403** (April 2010) 1392, hrefhttp://arxiv.org/abs/0906.4101arXiv:0906.4101.
78. E. G. P. Bos, R. van de Weygaert, K. Dolag and V. Pettorino, *MNRAS* **426** (October 2012) 440, hrefhttp://arxiv.org/abs/1205.4238arXiv:1205.4238 [astro-ph.CO].
79. P. M. Sutter, E. Carlesi, B. D. Wandelt and A. Knebe, *MNRAS* **446** (January 2015) L1, hrefhttp://arxiv.org/abs/1406.0511arXiv:1406.0511.
80. B. Li, *MNRAS* **411** (March 2011) 2615, hrefhttp://arxiv.org/abs/1009.1406arXiv:1009.1406 [astro-ph.CO].
81. B. Li, G.-B. Zhao and K. Koyama, *MNRAS* **421** (April 2012) 3481, hrefhttp://arxiv.org/abs/1111.2602arXiv:1111.2602 [astro-ph.CO].
82. J. Clampitt, Y.-C. Cai and B. Li, *MNRAS* **431** (2013) 749, hrefhttp://arxiv.org/abs/1212.2216arXiv:1212.2216 [astro-ph.CO].
83. T. Y. Lam, J. Clampitt, Y.-C. Cai and B. Li, *MNRAS* **450** (July 2015) 3319, hrefhttp://arxiv.org/abs/1408.5338arXiv:1408.5338.
84. P. Zivick, P. M. Sutter, B. D. Wandelt, B. Li and T. Y. Lam, *MNRAS* **451** (August 2015) 4215, hrefhttp://arxiv.org/abs/1411.5694arXiv:1411.5694.
85. G. Pollina, M. Baldi, F. Marulli and L. Moscardini, *MNRAS* **455** (January 2016) 3075, hrefhttp://arxiv.org/abs/1506.08831arXiv:1506.08831.
86. A. Barreira, M. Cautun, B. Li, C. M. Baugh and S. Pascoli, *jcap* **8** (August 2015) 028, hrefhttp://arxiv.org/abs/1505.05809arXiv:1505.05809.
87. E. Massara, F. Villaescusa-Navarro, M. Viel and P. M. Sutter, *jcap* **11** (November 2015) 018, hrefhttp://arxiv.org/abs/1506.03088arXiv:1506.03088.
88. L. F. Yang, M. C. Neyrinck, M. A. Aragón-Calvo, B. Falck and J. Silk, *mnras* **451** (August 2015) 3606, hrefhttp://arxiv.org/abs/1411.5029arXiv:1411.5029.
89. F.-S. Kitaura, C.-H. Chuang, Y. Liang, C. Zhao, C. Tao, S. Rodríguez-Torres, D. J. Eisenstein, H. Gil-Marín, J.-P. Kneib, C. McBride, W. J. Percival, A. J. Ross, A. G. Sánchez, J. Tinker, R. Tojeiro, M. Vargas-Magana and G.-B. Zhao, *Physical Review Letters* **116** (April 2016) 171301, hrefhttp://arxiv.org/abs/1511.04405arXiv:1511.04405.
90. Y. Liang, C. Zhao, C.-H. Chuang, F.-S. Kitaura and C. Tao, *MNRAS* **459** (July 2016) 4020, hrefhttp://arxiv.org/abs/1511.04391arXiv:1511.04391.
91. L. Hui, A. Nicolis and C. W. Stubbs, *Phys. Rev. D* **80** (November 2009) 104002, hrefhttp://arxiv.org/abs/0905.2966arXiv:0905.2966 [astro-ph.CO].
92. B. Li and H. Zhao, *Phys. Rev. D* **80** (August 2009) 044027,

hrefhttp://arxiv.org/abs/0906.3880arXiv:0906.3880 [astro-ph.CO].
93. B. Li and J. D. Barrow, *Phys. Rev. D* **83** (January 2011) 024007, hrefhttp://arxiv.org/abs/1005.4231arXiv:1005.4231 [astro-ph.CO].
94. B. Jain, *Philosophical Transactions of the Royal Society of London Series A* **369** (December 2011) 5081, hrefhttp://arxiv.org/abs/1104.0415arXiv:1104.0415.
95. B. Jain and J. VanderPlas, *jcap* **10** (October 2011) 032, hrefhttp://arxiv.org/abs/1106.0065arXiv:1106.0065.
96. G.-B. Zhao, B. Li and K. Koyama, *Physical Review Letters* **107** (August 2011) 071303, hrefhttp://arxiv.org/abs/1105.0922arXiv:1105.0922 [astro-ph.CO].
97. A. Cabré, V. Vikram, G.-B. Zhao, B. Jain and K. Koyama, *jcap* **7** (July 2012) 034, hrefhttp://arxiv.org/abs/1204.6046arXiv:1204.6046.
98. M. Sahlén, Í. Zubeldía and J. Silk, *ApJ* **820** (March 2016) L7, hrefhttp://arxiv.org/abs/1511.04075arXiv:1511.04075.
99. R. Voivodic, M. Lima, C. Llinares and D. F. Mota, *Phys. Rev. D* **95** (January 2017) 024018, hrefhttp://arxiv.org/abs/1609.02544arXiv:1609.02544.
100. DESI Collaboration, A. Aghamousa, J. Aguilar, S. Ahlen, S. Alam, L. E. Allen, C. Allende Prieto, J. Annis, S. Bailey, C. Balland and et al., *ArXiv e-prints* (October 2016) hrefhttp://arxiv.org/abs/1611.00036arXiv:1611.00036 [astro-ph.IM].
101. M. Sahlén and J. Silk, *ArXiv e-prints* (December 2016) hrefhttp://arxiv.org/abs/1612.06595arXiv:1612.06595.
102. E. V. Linder and R. N. Cahn, *Astroparticle Physics* **28** (December 2007) 481, hrefhttp://arxiv.org/abs/astro-ph/0701317astro-ph/0701317.
103. G. Pollina, N. Hamaus, K. Paech, K. Dolag, J. Weller, C. Sánchez, E. S. Rykoff, B. Jain, T. M. C. Abbott, S. Allam, S. Avila, R. A. Bernstein, E. Bertin, D. Brooks, D. L. Burke, A. Carnero Rosell, M. Carrasco Kind, J. Carretero, C. E. Cunha, C. B. D'Andrea, L. N. da Costa, J. De Vicente, D. L. DePoy, S. Desai, H. T. Diehl, P. Doel, A. E. Evrard, B. Flaugher, P. Fosalba, J. Frieman, J. García-Bellido, D. W. Gerdes, T. Giannantonio, D. Gruen, J. Gschwend, G. Gutierrez, W. G. Hartley, D. L. Hollowood, K. Honscheid, B. Hoyle, D. J. James, T. Jeltema, K. Kuehn, N. Kuropatkin, M. Lima, M. March, J. L. Marshall, P. Melchior, F. Menanteau, R. Miquel, A. A. Plazas, A. K. Romer, E. Sanchez, V. Scarpine, R. Schindler, M. Schubnell, I. Sevilla-Noarbe, M. Smith, M. Soares-Santos, F. Sobreira, E. Suchyta, G. Tarle, A. R. Walker and W. Wester, *ArXiv e-prints* (June 2018) hrefhttp://arxiv.org/abs/1806.06860arXiv:1806.06860.
104. D. Gruen, O. Friedrich, A. Amara, D. Bacon, C. Bonnett, W. Hartley, B. Jain, M. Jarvis, T. Kacprzak, E. Krause, A. Mana, E. Rozo, E. S. Rykoff, S. Seitz, E. Sheldon, M. A. Troxel, V. Vikram, T. M. C. Abbott, F. B. Abdalla, S. Allam, R. Armstrong, M. Banerji, A. H. Bauer, M. R. Becker, A. Benoit-Lévy, G. M. Bernstein, R. A. Bernstein, E. Bertin, S. L. Bridle, D. Brooks, E. Buckley-Geer, D. L. Burke, D. Capozzi, A. Carnero Rosell, M. Carrasco Kind, J. Carretero, M. Crocce, C. E. Cunha, C. B. D'Andrea, L. N. da Costa, D. L. DePoy, S. Desai, H. T. Diehl, J. P. Dietrich, P. Doel, T. F. Eifler, A. F. Neto, E. Fernandez, B. Flaugher, P. Fosalba, J. Frieman, D. W. Gerdes, R. A. Gruendl, G. Gutierrez, K. Honscheid, D. J. James, K. Kuehn, N. Kuropatkin, O. Lahav, T. S. Li, M. Lima, M. A. G. Maia, M. March, P. Martini, P. Melchior, C. J. Miller, R. Miquel, J. J. Mohr, B. Nord, R. Ogando, A. A. Plazas, K. Reil, A. K. Romer, A. Roodman, M. Sako, E. Sanchez, V. Scarpine, M. Schubnell, I. Sevilla-Noarbe, R. C. Smith, M. Soares-Santos, F. Sobreira, E. Suchyta, M. E. C. Swanson, G. Tarle, J. Thaler, D. Thomas, A. R. Walker, R. H. Wechsler, J. Weller, Y. Zhang and J. Zuntz, *MNRAS* **455** (January 2016) 3367, hrefhttp://arxiv.org/abs/1507.05090arXiv:1507.05090.

105. A. Barreira, S. Bose, B. Li and C. Llinares, *jcap* **2** (February 2017) 031, hrefhttp://arxiv.org/abs/1605.08436`arXiv:1605.08436`.
106. M. M. Brouwer, V. Demchenko, J. Harnois-Déraps, M. Bilicki, C. Heymans, H. Hoekstra, K. Kuijken, M. Alpaslan, S. Brough, Y.-C. Cai, M. V. Costa-Duarte, A. Dvornik, T. Erben, H. Hildebrandt, B. W. Holwerda, P. Schneider, C. Sifón and E. van Uitert, *ArXiv e-prints* (May 2018) hrefhttp://arxiv.org/abs/1805.00562`arXiv:1805.00562`.
107. O. Friedrich, D. Gruen, J. DeRose, D. Kirk, E. Krause, T. McClintock, E. S. Rykoff, S. Seitz, R. H. Wechsler, G. M. Bernstein, J. Blazek, C. Chang, S. Hilbert, B. Jain, A. Kovacs, O. Lahav, F. B. Abdalla, S. Allam, J. Annis, K. Bechtol, A. Benoit-Levy, E. Bertin, D. Brooks, A. Carnero Rosell, M. Carrasco Kind, J. Carretero, C. E. Cunha, C. B. D'Andrea, L. N. da Costa, C. Davis, S. Desai, H. T. Diehl, J. P. Dietrich, A. Drlica-Wagner, T. F. Eifler, P. Fosalba, J. Frieman, J. Garcia-Bellido, E. Gaztanaga, D. W. Gerdes, T. Giannantonio, R. A. Gruendl, J. Gschwend, G. Gutierrez, K. Honscheid, D. J. James, M. Jarvis, K. Kuehn, N. Kuropatkin, M. Lima, M. March, J. L. Marshall, P. Melchior, F. Menanteau, R. Miquel, J. J. Mohr, B. Nord, A. A. Plazas, E. Sanchez, V. Scarpine, R. Schindler, M. Schubnell, I. Sevilla-Noarbe, E. Sheldon, M. Smith, M. Soares-Santos, F. Sobreira, E. Suchyta, M. E. C. Swanson, G. Tarle, D. Thomas, M. A. Troxel, V. Vikram and J. Weller, *ArXiv e-prints* (October 2017) hrefhttp://arxiv.org/abs/1710.05162`arXiv:1710.05162`.
108. C. T. Davies, M. Cautun and B. Li, *MNRAS* **480** (October 2018) L101, hrefhttp://arxiv.org/abs/1803.08717`arXiv:1803.08717`.
109. T. Chantavat, U. Sawangwit and B. D. Wandelt, *ApJ* **836** (February 2017) 156, hrefhttp://arxiv.org/abs/1702.01009`arXiv:1702.01009`.
110. W. Hu and I. Sawicki, *Phys. Rev. D* **76** (Sep 2007) 064004.
111. T. Baker, J. Clampitt, B. Jain and M. Trodden, *Phys. Rev. D* **98** (July 2018) 023511, hrefhttp://arxiv.org/abs/1803.07533`arXiv:1803.07533`.
112. J. Renk, M. Zumalacárregui, F. Montanari and A. Barreira, *jcap* **10** (October 2017) 020, hrefhttp://arxiv.org/abs/1707.02263`arXiv:1707.02263`.
113. A. Barreira, B. Li, W. A. Hellwing, C. M. Baugh and S. Pascoli, *jcap* **10** (October 2013) 027, hrefhttp://arxiv.org/abs/1306.3219`arXiv:1306.3219`.
114. H. A. Winther and P. G. Ferreira, *Phys. Rev. D* **92** (September 2015) 064005, hrefhttp://arxiv.org/abs/1505.03539`arXiv:1505.03539 [gr-qc]`.
115. M. Cautun, E. Paillas, Y.-C. Cai, S. Bose, J. Armijo, B. Li and N. Padilla, *ArXiv e-prints* (October 2017) hrefhttp://arxiv.org/abs/1710.01730`arXiv:1710.01730`.
116. L. Lombriser, *Annalen der Physik* **264** (Aug 2014) 259, hrefhttp://arxiv.org/abs/1403.4268`arXiv:1403.4268 [astro-ph.CO]`.
117. E. Paillas, M. Cautun, B. Li, Y.-C. Cai, N. Padilla, J. Armijo and S. Bose, *MNRAS* **484** (March 2019) 1149, hrefhttp://arxiv.org/abs/1810.02864`arXiv:1810.02864`.
118. P. Zhang, M. Liguori, R. Bean and S. Dodelson, *Physical Review Letters* **99** (October 2007) 141302, hrefhttp://arxiv.org/abs/0704.1932`arXiv:0704.1932`.
119. R. Reyes, R. Mandelbaum, U. Seljak, T. Baldauf, J. E. Gunn, L. Lombriser and R. E. Smith, *Nature* **464** (March 2010) 256, hrefhttp://arxiv.org/abs/1003.2185`arXiv:1003.2185 [astro-ph.CO]`.
120. L. Lombriser, A. Slosar, U. Seljak and W. Hu, *Phys. Rev. D* **85** (June 2012) 124038, hrefhttp://arxiv.org/abs/1003.3009`arXiv:1003.3009`.
121. S. Alam, H. Miyatake, S. More, S. Ho and R. Mandelbaum, *MNRAS* **465** (March 2017) 4853, hrefhttp://arxiv.org/abs/1610.09410`arXiv:1610.09410`.
122. A. Amon, C. Blake, C. Heymans, C. D. Leonard, M. Asgari, M. Bilicki, A. Choi, T. Erben, K. Glazebrook, J. Harnois-Deraps, H. Hildebrandt, H. Hoekstra, B. Joachimi, S. Joudaki, K. Kuijken, C. Lidman,

D. Parkinson, E. A. Valentijn and C. Wolf, *ArXiv e-prints* (November 2017) hrefhttp://arxiv.org/abs/1711.10999arXiv:1711.10999.

123. S. Singh, S. Alam, R. Mandelbaum, U. Seljak, S. Rodriguez-Torres and S. Ho, *ArXiv e-prints* (March 2018) hrefhttp://arxiv.org/abs/1803.08915arXiv:1803.08915.
124. D. Spolyar, M. Sahlén and J. Silk, *Physical Review Letters* **111** (December 2013) 241103, hrefhttp://arxiv.org/abs/1304.5239arXiv:1304.5239 [astro-ph.CO].
125. N. Hamaus, P. M. Sutter, G. Lavaux and B. D. Wandelt, *jcap* **11** (November 2015) 036, hrefhttp://arxiv.org/abs/1507.04363arXiv:1507.04363.
126. S. Nadathur and W. J. Percival, *ArXiv e-prints* (December 2017) hrefhttp://arxiv.org/abs/1712.07575arXiv:1712.07575.
127. I. Achitouv, *Phys. Rev. D* **96** (October 2017) 083506, hrefhttp://arxiv.org/abs/1707.08121arXiv:1707.08121.
128. I. Achitouv and Y.-C. Cai, *ArXiv e-prints* (June 2018) hrefhttp://arxiv.org/abs/1806.04684arXiv:1806.04684.
129. I. Achitouv, C. Blake, P. Carter, J. Koda and F. Beutler, *Phys. Rev. D* **95** (April 2017) 083502, hrefhttp://arxiv.org/abs/1606.03092arXiv:1606.03092.
130. A. J. Hawken, B. R. Granett, A. Iovino, L. Guzzo, J. A. Peacock, S. de la Torre, B. Garilli, M. Bolzonella, M. Scodeggio, U. Abbas, C. Adami, D. Bottini, A. Cappi, O. Cucciati, I. Davidzon, A. Fritz, P. Franzetti, J. Krywult, V. Le Brun, O. Le Fèvre, D. Maccagni, K. Małek, F. Marulli, M. Polletta, A. Pollo, L. A. M. Tasca, R. Tojeiro, D. Vergani, A. Zanichelli, S. Arnouts, J. Bel, E. Branchini, G. De Lucia, O. Ilbert, L. Moscardini and W. J. Percival, *A&A* **607** (November 2017) A54, hrefhttp://arxiv.org/abs/1611.07046arXiv:1611.07046.
131. A. J. Ross, S. Ho, A. J. Cuesta, R. Tojeiro, W. J. Percival, D. Wake, K. L. Masters, R. C. Nichol, A. D. Myers, F. de Simoni, H. J. Seo, C. Hernández-Monteagudo, R. Crittenden, M. Blanton, J. Brinkmann, L. A. N. da Costa, H. Guo, E. Kazin, M. A. G. Maia, C. Maraston, N. Padmanabhan, F. Prada, B. Ramos, A. Sanchez, E. F. Schlafly, D. J. Schlegel, D. P. Schneider, R. Skibba, D. Thomas, B. A. Weaver, M. White and I. Zehavi, *MNRAS* **417** (October 2011) 1350, hrefhttp://arxiv.org/abs/1105.2320arXiv:1105.2320.
132. Y.-S. Song, H. Peiris and W. Hu, *Phys. Rev. D* **76** (September 2007) 063517, hrefhttp://arxiv.org/abs/0706.2399arXiv:0706.2399.
133. S. Ho, C. Hirata, N. Padmanabhan, U. Seljak and N. Bahcall, *Phys. Rev. D* **78** (August 2008) 043519, hrefhttp://arxiv.org/abs/0801.0642arXiv:0801.0642.
134. T. Giannantonio, R. Scranton, R. G. Crittenden, R. C. Nichol, S. P. Boughn, A. D. Myers and G. T. Richards, *Phys. Rev. D* **77** (June 2008) 123520, hrefhttp://arxiv.org/abs/0801.4380arXiv:0801.4380.
135. A. Kovács, *MNRAS* **475** (April 2018) 1777, hrefhttp://arxiv.org/abs/1701.08583arXiv:1701.08583.
136. A. J. Ross, W. J. Percival, A. G. Sánchez, L. Samushia, S. Ho, E. Kazin, M. Manera, B. Reid, M. White, R. Tojeiro, C. K. McBride, X. Xu, D. A. Wake, M. A. Strauss, F. Montesano, M. E. C. Swanson, S. Bailey, A. S. Bolton, A. M. Dorta, D. J. Eisenstein, H. Guo, J.-C. Hamilton, R. C. Nichol, N. Padmanabhan, F. Prada, D. J. Schlegel, M. V. Magaña, I. Zehavi, M. Blanton, D. Bizyaev, H. Brewington, A. J. Cuesta, E. Malanushenko, V. Malanushenko, D. Oravetz, J. Parejko, K. Pan, D. P. Schneider, A. Shelden, A. Simmons, S. Snedden and G.-b. Zhao, *MNRAS* **424** (July 2012) 564, hrefhttp://arxiv.org/abs/1203.6499arXiv:1203.6499.
137. A. J. Ross, F. Beutler, C.-H. Chuang, M. Pellejero-Ibanez, H.-J. Seo, M. Vargas-Magaña, A. J. Cuesta, W. J. Percival, A. Burden, A. G. Sánchez, J. N. Grieb, B. Reid, J. R. Brownstein, K. S. Dawson, D. J. Eisenstein, S. Ho, F.-

S. Kitaura, R. C. Nichol, M. D. Olmstead, F. Prada, S. A. Rodríguez-Torres, S. Saito, S. Salazar-Albornoz, D. P. Schneider, D. Thomas, J. Tinker, R. Tojeiro, Y. Wang, M. White and G.-b. Zhao, *MNRAS* **464** (January 2017) 1168, hrefhttp://arxiv.org/abs/1607.03145`arXiv:1607.03145`.